Hettiwatte, S.N., Cowan, B.R. and Young, A.A. (2007) Generalized Analysis Framework for SPAMM, HARP and DENSE. In: Proceedings of the Society for Cardiovascular Magnetic Resonance 2007. Journal of Cardiovascular Magnetic Resonance, Vol. 9, No. 2, pp. 354-355.

Ronald J. Beyers, MSEE, Yaqin Xu, MD, PhD, Stuart S. Berr, PhD, Frederick H. Epstein, PhD, Joel Linden, PhD, Brent A. French, PhD. ***University of Virginia, Charlottesville, VA, USA.***

Introduction: CMR-based studies have previously demonstrated that potent agonists of the adenosine A2A Receptor (A2AR) can help preserve left ventricular (LV) contractile function early after reperfused myocardial infarction (MI) in mice (1). However, the long term effects of such anti-inflammatory agents on the progression of LV remodeling have not been explored, nor have the long-term effects of these agents ever been compared with the most effective clinical treatment regimen currently available – the combination of ACE-inhibition and beta-adrenergic receptor blockade (AI + BB).

Purpose: The purpose of this study was to test the hypothesis that selective A2AR activation could help preserve cardiac structure and function after reperfused MI similar to that provided by the combination of AI+BB.

Methods: All mice were studied by CMR before and at 1, 7, and 28 days after experimental MI. MI was induced by a 1 h occlusion of the LAD followed by reperfusion. Study groups were composed of untreated C57Bl/6J wild-type mice (WT, n = 6), mice treated with ATL313 (a potent A2AR agonist, n = 5) and mice treated with the combination AI + BB (n = 7). ATL313 was administered (10 ng/kg-min) starting 1h post-reperfusion until Day 14 post-MI using implanted Alzet micro-osmotic pumps (Durect Corp). The AI + BB combination of Captopril and Metoprolol (each at 35 ug/kg-min) was delivered similarly starting 1 h post-reperfusion until Day 28. CMR studies included localizer scanning, 6-8 short-axis slices of black-blood cine imaging to cover the entire heart, and at Day 1, 6–7 gadolinium-enhanced, high flip-angle (60–90°) short-axis slices. Gd-DTPA was infused after cine imaging through an indwelling IP line. All imaging was performed on a 4.7 T scanner with a custom-built Litz RF-coil (Doty Scientific). All images had a field-of-view of 2.56 cm, a matrix size of 128 × 128, and zero-filled pixel size of 0.1 × 0.1 mm^2. Post acquisition analysis performed on Matlab yielded myocardial LV end-diastolic (ED), end-systolic (ES) volumes and ejection fraction (EF) from the cine images. Day 1 infarct size was measured as percent of LV mass from the gadolinium enhanced images.

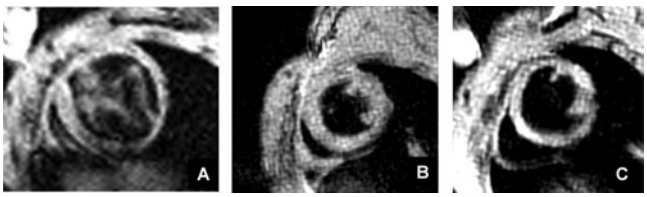

FIG. 1. Mid-ventricular short-axis images 28 days post-MI of (A) an untreated WT mouse, (B) a WT mouse treated with ATL-313, an (C) a WT mouse treated with AI+BB. Reduced cavity ize and circumferential extent of all thinning are evident in (B) and (C).

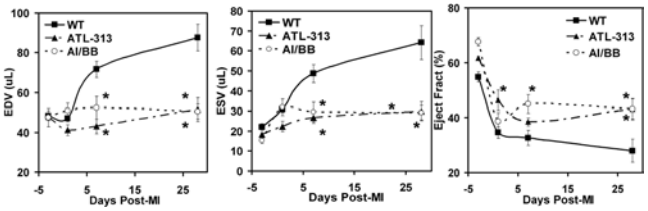

FIG. 2. End diastolic volume (EDV), end systolic volume (ESV) and jection fraction (EF) at baseline and during first 28 days following MI. Selective activation of the A2AR (ATL-313) reduces ESV and increases EF to a degree similar to that seen in Al+BB mice compared to untreated wild-ty;e (WT) mice. Note * indicates $p<0.05$ in comparison to WT.

Results: Gadolinium-enhanced CMR demonstrated similar Day 1 infarct sizes in untreated (40 ± 4%), ATL313-treated (41 ± 3%) and AI+BB-treated mice (44 ± 5%) with p = NS by ANOVA. Fig. 1 shows example Day 28 ED images illustrating the effect of drug treatments. Specifically, LV cavity dilation and circumferential wall thinning are evident in the untreated mice (Fig. 1A). In contrast, preservation of cavity size and minimal wall-thinning in the anterior segment were seen in the ATL313- and AI + BB-treated groups (Figs. 1B&C). Fig. 2 shows the EDV, ESV and EF results from the present study. Both ATL313 and AI+BB significantly reduced both EDV and ESV at Days 7 and 28 post-MI compared to WT. ATL313 improved EF on Days 1 and 28 post-MI, whereas AI + BB improved EF on Days 7 and 28 post-MI. All comparisons reported here met $p < 0.05$ by ANOVA.

Conclusions: Using CMR, we have shown that selective activation of the A2AR reduces post-infarct LV remodeling to an extent similar to that provided by the combination of ACE-inhibition and beta-adrenergic receptor blockade. In addition, A2AR-stimulation preserves EF on Day 1 post-MI significantly better than the combination of AI + BB, a property that may prove beneficial to survival in patients with large anterior MI. More generally, these results demonstrate the utility of serial CMR in mice for evaluating the efficacy of new therapies against heart failure and for comparing new therapeutic approaches with conventional clinical paradigms.

REFERENCE

1. Toufektsian MC, Yang Z, Prasad KM, Overbergh L, Ramos SI, Mathieu C, Linden J, and French BA. Stimulation of A2A-adenosine receptors after myocardial infarction suppresses inflammatory activation and attenuates contractile dysfunction in the remote left ventricle. AJP Heart & Circ Phys 2006; 290:H1410–1418.

508. GENERALIZED ANALYSIS FRAMEWORK FOR SPAMM, HARP AND DENSE

Sujeewa N. Hettiwatte, PhD,[1] Brett R. Cowan, MBChB,[2] Alistair A. Young, PhD.[3] ***[1]Bioengineering Institute, University of Auckland, Auckland, New Zealand, [2]Centre***

for Advanced MRI, Faculty of Medical and Health Sciences, University of Auckland, Auckland, New Zealand, [3]Department of Anatomy with Radiology and Bioengineering Institute, University of Auckland, Auckland, New Zealand.

Introduction: A number of MR imaging techniques are used to measure deformation in the heart including SPAtial Modulation of Magnetization (SPAMM), HARmonic Phase (HARP) and Displacement ENcoding using Stimulated Echoes (DENSE). In SPAMM, a line or grid tag pattern is created magnetically in the tissue and displacement is measured from this reference by tracking the tags. In HARP, position information is encoded into the phase of a filtered image and this is used to calculate displacement. In DENSE, displacements are directly encoded into the phase of the image.

Purpose: We show how all methods can be analyzed using a single generalized framework. We test this framework by numerically creating SPAMM, HARP and DENSE images with known deformations and comparing the results with the analytical solution.

Methods: A known deformation was defined comprising axial shear in a cylindrical annulus (1). SPAMM grid-tagged images were generated with a tag spacing of 7 mm at 45 deg and 135 deg with the first five terms of a Fourier expansion used to approximate a square wave tag profile. CSPAMM cosine modulated images and DENSE images were generated with displacement encoding in both the × and y directions. All images were generated in DICOM format; SPAMM and CSPAMM at 256 × 256 and DENSE at 128 × 128 resolution, all with FOV = 300 mm.

Displacement images were calculated as follows. In SPAMM, grid tagged images were interpolated to 512 × 512, and convolved with a 2nd derivative of a Gaussian to obtain line tags in each direction. Tags were detected by searching from each pixel along a line normal to the initial undeformed tags. Each pixel value was equated to the distance from that pixel to the nearest tag centre in the tag direction to obtain a wrapped image of initial position X as a function of current position x. The displacement u(x) was then given by x-X(x). This displacement is only accurate at tag line centers; at other points displacement was obtained using a thin plate spline interpolation. In HARP, the Fourier transform of CSPAMM images gave spectral peaks, which were filtered using a circular filter centered at the harmonic peak d = 1/7 cycles/mm with radius 0.8 d and Gaussian roll off. The phase of the inverse Fourier transform gave the X(x) map, and displacement u(x) was again given by x-X(x). In DENSE, the image phase gave displacement u(x) directly. The displacement maps from each method were unwrapped (2) and used to calculate angular and radial displacements and Eulerian strains, using the same pixel based calculation.

Results: The figure shows the unwrapped displacement maps from each technique in the × and y directions. The mean and standard deviation of differences with the analytic solution were calculated for all pixels at least 5 mm from the inner or outer edge (Table).

Conclusions: A generalized analysis framework demonstrates the similarity in displacement encoding methods. Simulated errors in displacements and strains were lowest in DENSE, intermediate in HARP and highest in SPAMM. SPAMM had the highest errors due to the simple pixel based tracking algorithm and the interpolation scheme used. In HARP, the errors are largely due to the choice of filter parameters used in Fourier domain.

REFERENCES

1. Radiology 1993; 188:101–108.
2. J Opt Soc Am A 1994; 11:107–117.

TABLE
Errors (mean ± sd) in displacement and Eulerian strains

	Angular displacement (degrees)	Radial displacement (mm)	Radial strain	Circumferential strain	Shear strain
SPAMM	−1.88 ± 0.46	−0.35 ± 0.29	0.00 ± 0.07	−0.01 ± 0.02	0.03 ± 0.03
HARP	1.11 ± 0.77	0.06 ± 0.07	0.05 ± 0.05	0.00 ± 0.00	−0.04 ± 0.02
DENSE	0.00 ± 0.01	0.00 ± 0.01	0.00 ± 0.00	0.00 ± 0.00	0.00 ± 0.00

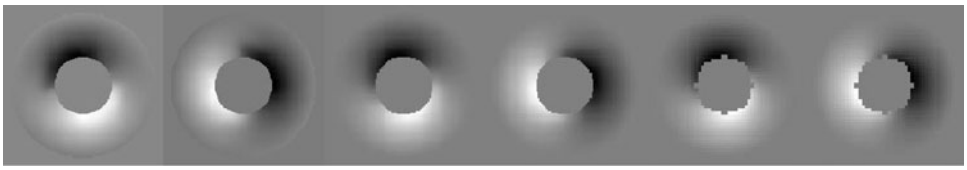

FIG. 1. Unwrapped displacement maps: Left to right: SPAMM (x and y), HARP(x and y) and DENSE (x and y).